World Journal of Nephrology

Submit a Manuscript: http://www.f6publishing.com

World J Nephrol 2018 September 7; 7(5): 108-116

DOI: 10.5527/wjn.v7.i5.108

ISSN 2220-6124 (online)

ORIGINAL ARTICLE

Basic Study

Unique interstitial miRNA signature drives fibrosis in a murine model of autosomal dominant polycystic kidney disease

Ameya Patil, William E Sweeney Jr, Cynthia G Pan, Ellis D Avner

Ameya Patil, William E Sweeney Jr, Cynthia G Pan, Ellis D Avner, Children's Research Institute; Children's' Hospital Health System of Wisconsin and the Medical College of Wisconsin, Milwaukee, WI 53226, United States

ORCID number: Ameya Patil (0000-0003-4666-2205); William E Sweeney Jr (0000-0001-9375-2348); Cynthia G Pan (0000-0002-1181-0901); Ellis D Avner (0000-0002-6734-1884).

Author contributions: Patil A, Sweeney Jr WE, Pan CG and Avner ED all equally contributed to the conception and design of this study, analysis, and interpretation of data; all authors drafted the article and made critical revisions related to the intellectual content of the manuscript, and approved the final version of the article to be published.

Supported by the Children's Research Institute, the Lillian Goldman Charitable Trust; Amy P Goldman Foundation; and Ellsworth Family and Children's Foundation of Children's' Hospital and Health System of Wisconsin.

Institutional animal care and use committee statement: All animal experiments are conducted in accordance with policies of the NIH Guide for the Care and Use of Laboratory Animals and the Institutional Animal Care and Use Committee (IACUC) of the Medical College of Wisconsin. The IACUC at the Medical College of Wisconsin is properly appointed according to PHS policy Ⅳ.A.3.a and is qualified through the experience and expertise of its members to oversee the Institution's animal care and use program. The Animal Welfare Assurance for the Medical College of Wisconsin is A3102-01. Specific protocols used in this study were approved by the Medical College of Wisconsin IACUC (approved protocols are AUA 4278 and AUA 4179).

Conflict-of-interest statement: The authors have no conflict of interest to declare. Conflict of Interest in Research statements is on file with the institution as per Medical College of Wisconsin policy #RS.GN.020.

Data sharing statement: Data sets and statistical methods are available upon request from the corresponding author

ARRIVE guidelines statement: The manuscript was revised according to the ARRIVE guidelines.

Manuscript source: Unsolicited manuscript

Correspondence to: Ameya P Patil, MD, Assistant Professor, Department of Pediatrics, Medical College of Wisconsin, Children's Research Institute, Children's' Hospital Health System of Wisconsin, Children's Corporate Center, Suite 510, Mailstop CCC C510, 999 North 92nd Street, Milwaukee, WI 53226, United States. appatil@mcw.edu
Telephone: +1-414-9555773
Fax: +1-414-3377105

Received: April 21, 2018
Peer-review started: April 21, 2018
First decision: May 16, 2018
Revised: May 25, 2018
Accepted: July 31, 2018
Article in press: August 1, 2018
Published online: September 7, 2018

Abstract

AIM

To delineate changes in miRNA expression localized to the peri-cystic local microenvironment (PLM) in an orthologous mouse model of autosomal dominant

polycystic kidney disease (ADPKD) (*mcwPkd1*$^{(nl/nl)}$).

METHODS

We profiled miRNA expression in the whole kidney and laser captured microdissection (LCM) samples from PLM in *mcwPkd1*$^{(nl/nl)}$ kidneys with Qiagen miScript 384 HC miRNA PCR arrays. The three times points used are: (1) post-natal (PN) day 21, before the development of trichrome-positive areas; (2) PN28, the earliest sign of trichrome staining; and (3) PN42 following the development of progressive fibrosis. PN21 served as appropriate controls and as the reference time point for comparison of miRNA expression profiles.

RESULTS

LCM samples revealed three temporally upregulated miRNAs [2 to 2.75-fold at PN28 and 2.5 to 4-fold ($P \leqslant 0.05$) at PN42] and four temporally downregulated miRNAs [2 to 2.75 fold at PN28 and 2.75 to 5-fold ($P \leqslant 0.05$) at PN42]. Expression of twenty-six miRNAs showed no change until PN42 [six decreased (2.25 to 3.5-fold) ($P \leqslant 0.05$) and 20 increased (2 to 4-fold) ($P \leqslant 0.05$)]. Many critical miRNA changes seen in the LCM samples from PLM were not seen in the contralateral whole kidney.

CONCLUSION

Precise sampling with LCM identifies miRNA changes that occur with the initiation and progression of renal interstitial fibrosis (RIF). Identification of the target proteins regulated by these miRNAs will provide new insight into the process of fibrosis and identify unique therapeutic targets to prevent or slow the development and progression of RIF in ADPKD.

Key words: Inflammation; End-stage renal disease; Cysts; Autosomal dominant polycystic kidney disease; miRNA; Renal interstitial fibrosis

Core tip: An essential and consistent histologic feature of progressive autosomal dominant polycystic kidney disease (ADPKD) is interstitial inflammation and fibrosis. This study investigated miRNA expression in local peri-cystic areas between cysts that become fibrotic as the disease progresses. This study identifies a critical limitation to whole organ transcriptomic approaches and demonstrates that laser capture microdissection (LCM) provides a means to overcome the dilutional factor of whole organ miRNA analysis. The precision of LCM provides a unique miRNA signature, which identifies novel molecular and therapeutic targets that initiate and drive interstitial fibrosis in ADPKD.

Patil A, Sweeney Jr WE, Pan CG, Avner ED. Unique interstitial miRNA signature drives fibrosis in a murine model of autosomal dominant polycystic kidney disease. *World J Nephrol* 2018; 7(5): 108-116 Available from: URL: http://www.wjgnet.com/2220-6124/full/v7/i5/108.htm DOI: http://dx.doi.org/10.5527/wjn.v7.i5.108

INTRODUCTION

Autosomal dominant polycystic kidney disease (ADPKD) is characterized by bilateral fluid-filled tubular cysts and progressive renal interstitial fibrosis (RIF). Renal function remains relatively normal until RIF reaches a tipping point, initiating a rapid decline of function leading to end-stage renal disease (ESRD).

miRNAs play key roles in diverse biological processes including cell division and death, intracellular signaling, cellular metabolism, immunity, and RIF. miRNAs are known to be involved in a variety of common human disorders including RIF[1, 2].

ADPKD is a common life-threatening renal disease that affects an estimated 12 million patients worldwide[3]. ADPKD is a heterogenetic disease with mutations in *PKD1* (MIM173910) (16p13.3) and *PKD2* (MIM173900) (4q22.1), which are responsible for approximately 80% and 15% cases respectively, with the remaining cases due to mutations at other rare loci[4].

Although ADPKD is a systemic disorder, it is characterized by the progressive development and growth of bilateral fluid-filled tubular cysts[5,6]. Renal cyst formation and expansion is followed by the development of RIF that ultimately leads to ESRD. Half of all ADPKD patients develop ESRD and require renal replacement therapy by their fifth decade[5,7].

Therapies currently in clinical trials focus on increased total kidney volume (TKV) as an indicator of disease severity, with decreased TKV reflecting the success of treatment[8-10]. However, an essential feature of the disease is interstitial inflammation and fibrosis[11-13]. Such interstitial changes lead to decreased TKV and strongly correlate with a decline in kidney function.

Renal fibrosis is the key determinant of the progression of all renal disease including ADPKD, irrespective of the original cause, and dictates the eventual outcome[11,13,14]. As cystic lesions enlarge, they compress both normal renal parenchyma and vascular elements between multiple cysts, creating a peri-cystic local microenvironment (PLM) that becomes fibrotic over time. The decline of renal function and the development of ESRD correlate with the progression of fibrosis in ADPKD[13,15,16]. Despite this link of ESRD to fibrosis, there is virtually no therapy specifically targeting fibrosis in ADPKD. This unmet clinical need calls for additional studies and a better understanding of the underlying mechanistic changes that lead to renal fibrosis.

Recent published studies have identified an essential role for miRNAs in the pathogenesis of both cyst formation and fibrosis in polycystic kidney disease[17-21]. miRNAs are short noncoding RNAs that regulate gene expression by reducing the translation of messenger RNAs[22-24]. miRNAs function in a diverse range of biological processes

and demonstrate spatial and temporal expression patterns[25]. MicroRNAs have been associated with many basic cellular processes as well as with a wide spectrum of diseases[1,24,25]. In the kidneys, miRNAs have been associated with renal development, homeostasis, and physiological functions[24,25]. Aberrant miRNA expression has been observed in mouse models of kidney fibrosis[18,20,26]. Notably, all previously published analysis has been performed in either whole kidney or cell culture models.

As cysts develop and enlarge, a local interstitial microenvironment is created between enlarging tubular cysts. This PLM is a complex milieu that integrates reciprocal signals from resident interstitial cells, infiltrating immune cells and proliferating cystic epithelial cells from enlarging tubular cysts. A complex interplay of many factors, including those driven by miRNA expression, occurs within the PLM. miRNAs play a role in determining the balance between pro-fibrotic and anti-fibrotic factors and how the dynamics of this balance drive the development of fibrosis[18,26]. In this study, we delineate changes in miRNA expression localized to the PLM in an orthologous mouse model of ADPKD (*mcwPkd1*$^{(nl/nl)}$). This model reliably demonstrates two phases of PKD: (1) the development and progressive enlargement of renal cysts, and (2) the development and progression of RIF, leading to loss of renal function. This model has a stable genetic background and permits both the investigation of pathogenic mechanisms and testing of potential therapeutic interventions. In the current study, we identify a unique PLM miRNA signature that drives fibrosis in this model.

MATERIALS AND METHODS

ADPKD mouse model (mcwPkd1$^{(nl/nl)}$*)*

The *mcwPkd1*$^{(nl/nl)}$ mice were generated as previously described[27]. Briefly, insertion of a neo-cassette into the Pkd1 allele (Pkd1nl) resulted in a cryptic splice site that allowed approximately 20% expression of a normal Pkd1 allele in homozygous *Pkd1*$^{(nl/nl)}$ mice[27]. In contrast to homozygous Pkd1 knockout mice, which are embryonically lethal, homozygous *mcwPkd1*$^{(nl/nl)}$ mice are viable, with bilaterally-enlarged polycystic kidneys by postnatal (PN) day 21, followed by the development and progression of RIF and ESRD between PN120 and PN150.

In the *mcwPkd1*$^{(nl/nl)}$ mouse, renal cystic lesions begin in utero, and TKV peaks by PN35. The initial appearance of light, wispy trichrome staining occurs in PLM at PN28.

All animal experiments were conducted in accordance with policies of the NIH Guide for the Care and Use of Laboratory Animals and the Institutional Animal Care and Use Committee (IACUC) of the Medical College of Wisconsin. The protocols used in this study were conducted under AUA 4379, which was approved by the Medical College of Wisconsin IACUC committee. The Animal Welfare Assurance for the Medical College of Wisconsin is A3102-01.

Sample preparation

Characterization of *mcwPkd1*$^{(nl/nl)}$ identified the time points of interest for this study. Triplicate samples from each of three time points were collected for analysis. These time points include: PN21, before evidence of collagen deposition with trichrome (controls); PN28, where trichrome-positive PLM was first evident; and PN42, when fibrosis was widespread. One kidney was placed directly in 10% formalin and paraffin-embedded (FFPE), and the contralateral kidney was flash frozen for RNA isolation.

Laser capture microdissection (LCM)

Serial 10 μm sections, at three different depths of the FFPE tissue, were floated onto PEN® membrane slides (Zeiss-415190-9081-000). A section from each of the three groups was stained lightly with McLethie's Trichrome stain for fibrosis. This stained section was used to guide LCM of its serial companion section. LCM of PN21 was accomplished by taking areas between multiple cysts due to the absence of trichrome-positive areas. The PN21 pre-fibrotic cystic kidney was used as the appropriate control, because aged-matched wildtype kidney is devoid of adequate interstitial areas for comparitive analysis (Figure 1).

RNA extraction

After harvesting 300000 um² of PLM, total (miRNA and mRNA) RNA was extracted with Qiagen's miRNeasy FFPE kit (Qiagen #217504) according to the manufacturer's instructions. The isolated total RNA was converted to cDNA using the miScript Ⅱ RT Kit (Qiagen #218161), according to the manufacturer's instructions, and was subsequently amplified using the miScript PreAMP PCR kit (Qiagen #331452). The amplified cDNA was used for reverse transcription PCR using the miRNome miScript miRNA PCR Array (Qiagen #331222) to assess changes in miRNA expression over time. miRNA profiling of contralateral whole kidney samples was similarly performed as described above.

Quality control

The quality of the samples was assessed by determining the 260/280 ratios and RNA integrity numbers (RIN) using the Agilent 2100 bioanalyzer and RNA 6000 Pico kits, respectively. RNA samples with a 260/280 ratio > 1.6 yielded an RIN between 7 and 9. RINs > 7 passed the internal RNA quality control test of the Qiagen miRNA plates. Samples with a 260/280 ratio > 1.6 were analyzed immediately and had to pass the internal controls of the plates to be included in our analysis. The RIN of the samples was periodically obtained. In all cases where the 260/280 ratio exceeded 1.6, RIN values

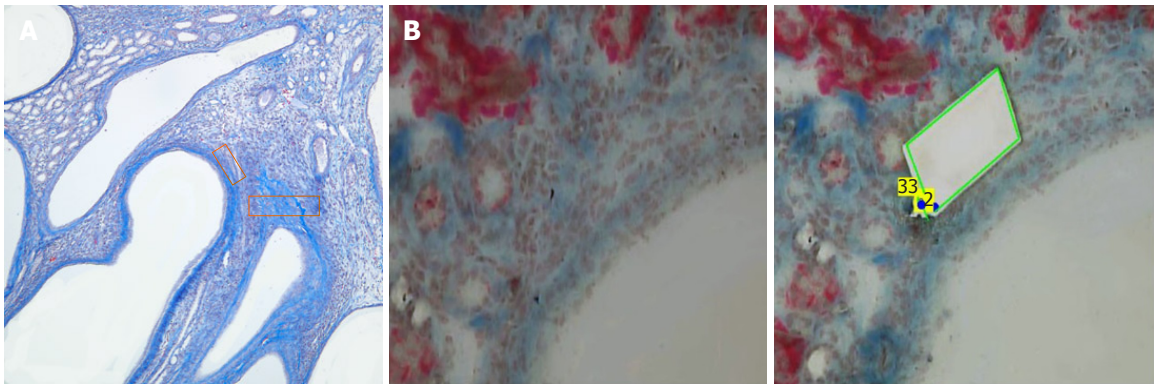

Trichrome stained section of ADPKD kidney | Pre-LCM | Post-LCM

Figure 1 Laser capture microdissection of the peri-cystic local microenvironment. A: Trichrome-stained section of a dominant polycystic kidney diseased (ADPKD) kidney with representative laser capture microdissection (LCM) areas marked by red rectangles; B: Trichrome-stained section of an ADPKD kidney before and after LCM.

exceeding 7.0 were obtained and passed the internal controls of the Qiagen plates.

Trichrome staining

Slides were deparaffinized in xylene, then rehydrated in 95% ETOH. Slides were then stained with McLethie's Trichrome (Newcomer Supply #9177), according to the manufacturer's instructions.

Statistical analysis

A total of three animals were included at each time point (PN21, PN28 and PN42) for both the LCM and whole kidney groups. Data were normalized for miRNA expression to stably-expressed housekeeping genes (*SNORD68* and *SNORD96A*) at each time point. Whole kidney miRNAs from contralateral kidneys were similarly examined at PN21, PN28 and PN42.

Average CT values and the standard deviations for the miRNAs expressed were examined. A sample size of $n = 3$, sufficient for appropriate statistical analysis, was selected. Data was analyzed using the Qiagen® online portal and GraphPad® Instat 3. Data are expressed as a change in expression for a particular miRNA (fold-regulation) at PN28 and PN42 compared to PN21 for both the PLM region and whole kidney. Only changes +/- 2-fold are included in the analysis. $P \leqslant 0.05$ was considered significant.

TargetScan and miRDB websites were used to determine targets for the miRNAs.

RESULTS

More than 900 miRNAs were examined in the laser captured PLM at the three different time points (PN21, PN28, PN42). miRNA expression in PLM at two different time points (PN28 and PN42) was compared with PN21 in order to: (1) provide a relative change in the expression of miRNAs during the onset of fibrosis; and (2) reflect local micro-environmental changes with disease progression.

Whole kidney miRNA changes compared with PLM miRNA changes

Whole kidney miRNA expression was compared to the miRNA expression profiles obtained from laser captured PLM samples at PN28 and PN42, with PN21 as a control (Figure 2). The heat maps show major differences in the expression levels of key miRNAs between the whole kidney and PLM areas (Figure 2).

PLM miRNA changes with onset of fibrosis at PN28

The mechanism(s) by which miRNAs represses translation allows us to make certain predictions. An increase in miRNA expression would likely lead to a reduction in the level of the target protein, and a decrease in miRNA expression would yield an increase in the target protein.

In Figure 3A, there are three miRNAs that show temporal increase in expression at PN28 and PN42. miR-667-3p, miR-3074-5p and miR-7b-3p are upregulated 2 to 2.75-fold at PN28, and are further upregulated to 2.5 to 4-fold and reach statistical significance at PN42.

In Figure 3B, a similar comparison made for sequentially downregulating miRNAs shows that a total of four miRNAs that are downregulated at PN28 continue to further decrease expression at PN42. miR-378a-3p, miR-30e-5p, miR-30a-5p and miR-344f-5p are downregulated 2 to 2.75-fold at PN28, and are further reduced 2.75 to 5-fold and reach statistical significance at PN42.

PLM miRNA changes with progressive fibrosis at PN42

Figure 4 show the results of PLM miRNA changes at PN42, which represents a stage of progressive fibrosis.

miRNAs with decreased expression > 2-fold at PN42 are shown in Figure 4A. miR-484, miR-455-3p, miR-130a-3p, miR-93-5p, miR-106-5p and miRN-677-3p are significantly downregulated in the range of 2.25 to 3.5-fold. miR-106-5p showed the largest decrease at 3.5-fold.

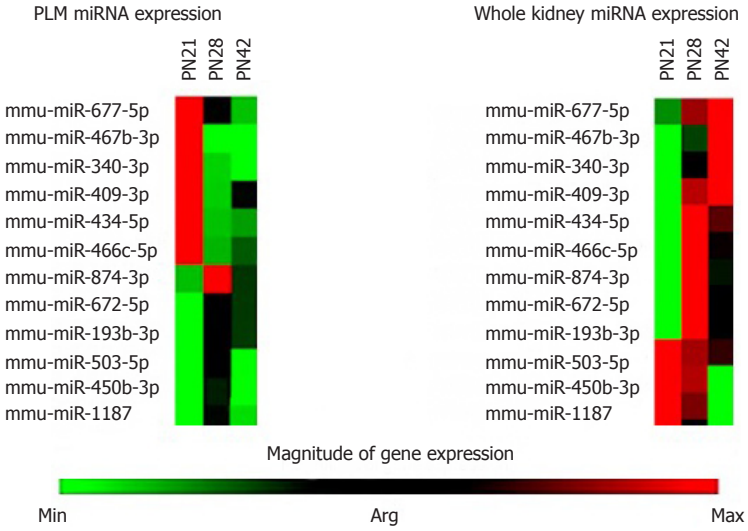

Figure 2 Heat map comparing miRNA expression. Heat map showing comparative expression of a set of miRNAs at three different post-natal (PN) time points (PN21, PN28 and PN42) for peri-cystic local microenvironmental regions and whole kidney samples (green represents downregulated miRNA expression, whereas red represents upregulated miRNA expression).

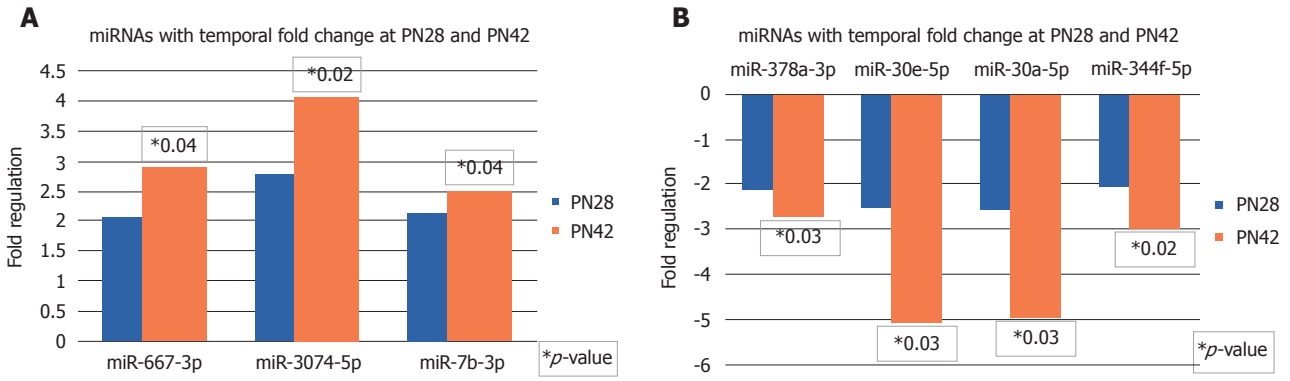

Figure 3 miRNA expression profiles. Expression profiles of a set of miRNAs at PN28 and PN42 that are temporally upregulated (A) and downregulated (B) when compared with PN21 in peri-cystic local microenvironmental regions.

miRNAs with increased expression >2-fold at PN42 are shown in Figure 4B. miR-409-3p, miR-762, miR-298-5p, miR-149-5p, miR-186-5p, miR-125a-3p, mIR-331-3p, miR-155-5p, miR-329-3p, miR-186-5p, miR-376c-3p, miR-665-3p, miR-383-5p, miR-107-3p, miR-542-3p, miR-672-5p, miR-32-5p, miR-96-5p, miR-503-5p and miR-466d-3p are significantly upregulated (2 to 4-fold).

DISCUSSION

In ADPKD, despite massive increases in kidney size, loss of renal function and progression to ESRD is largely dependent upon the development of renal fibrosis[11]. In the *mcwPkd1*$^{(nlnl)}$ mouse, we discovered that fibrosis started in discreet areas between multiple cysts at PN28, evidenced by light wispy trichrome-positive staining in sporadic areas between multiple cysts. Similar areas between multiple cysts were evident in PN21 kidneys, but they never showed positive trichrome staining. By PN42, trichrome staining revealed a spread of the fibrosis outward from PLM. This suggested to us that we may be able to identify critical elements necessary for the initiation and progression of fibrosis by using LCM to capture and analyze changes in PLM areas at the specific time-points noted. PN21 PLM areas provided appropriate controls, as they are devoid of fibrosis. Wild-type tissue was not an appropriate control in this experiment because it has minimal interstitial tissue that can be targeted for LCM. The risk of contaminating the wild-type LCM samples with epithelial tissue is unacceptably high.

Many previous studies have examined miRNA expression in whole kidneys to study progressive renal diseases[18,21,28-30]. However, a critical limitation to transcriptomic approaches of whole kidney is the kidney's cellular complexity: arrays from whole kidney reflect the averaged= expression of 26 or more different cell types[31-33]. This limitation is exacerbated in the presence of inflammatory cells in diseased kidneys.

The most striking result of these studies was the difference in miRNA profiles from PLM and whole kidney as shown in cluster heat maps (Figure 2). The expression of miRNAs in PLM is very different when compared to

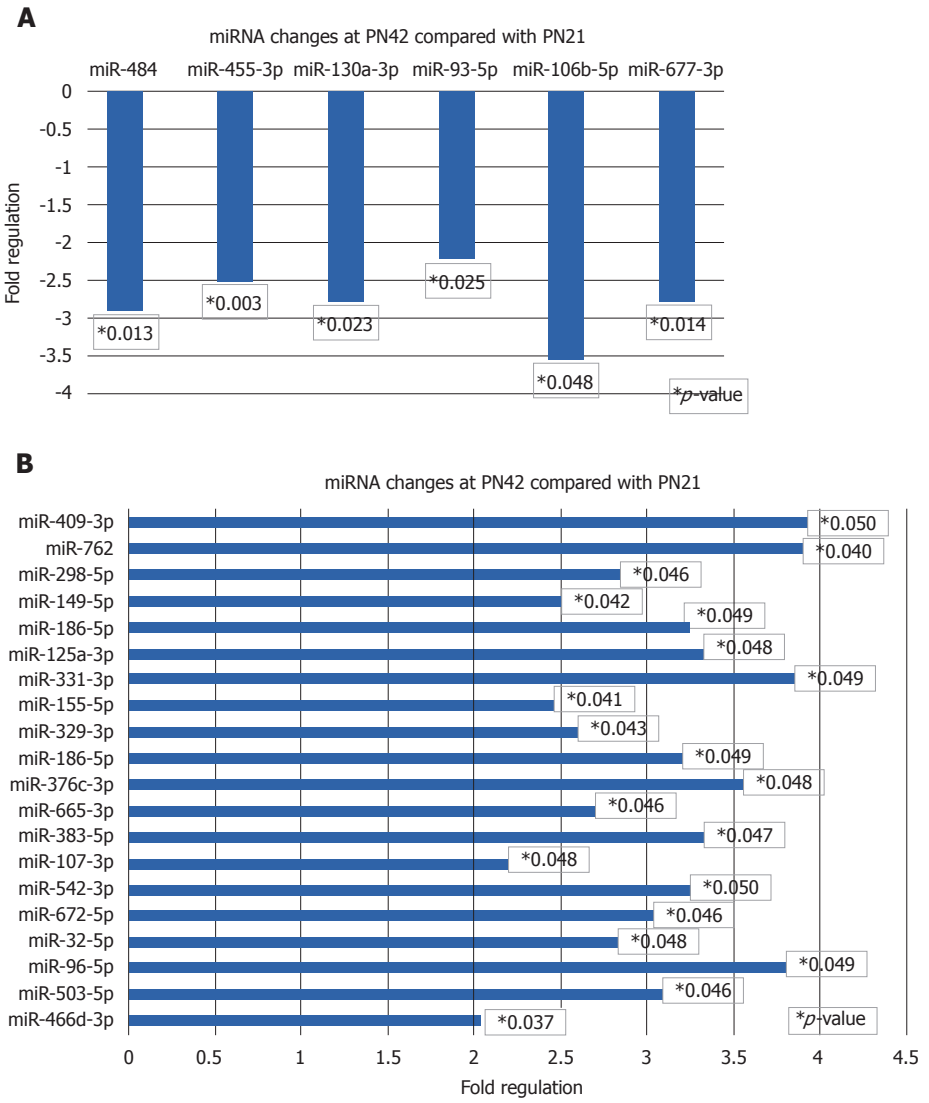

Figure 4 miRNA expression profiles. Expression profiles of a set of miRNAs with significantly decreased (A) and increased (B) expression at PN42 in peri-cystic local microenvironmental regions compared with PN21.

whole kidney expression. These findings likely reflect a dilution of important local changes in miRNAs when whole kidney comparisons are made. The implication of this is clear. Relying on whole kidney analysis may lead one to make errors in interpreting miRNA data.

The key miRNA changes noted in PLM, interestingly, are involved in or have predicted targets that play a role in the pathogenesis of either fibrosis, PKD or are unique. miRNAs with decreased expression at PN28 and PN42 (Figure 3B) have predicted targets (listed in brackets) as follows: miR-30a-5p and miR-30e-5p (Socs6, Timp2, Rock2, Bcl6, Col9a3, Col13a1, Smad1, Irf4) and miR-378a-3p (Mapk). Timp2 inhibits extracellular matrix proteolysis in multiple tissues, thus promoting fibrosis. Rock2, Irf4 and BCL6 have known roles in macrophage polarization, which plays an important role in the process of both inflammation and fibrosis. Mapk is an important mediator in the pathogenesis of PKD[34]. The expression of these miRNAs sequentially decreases at PN28 and PN42, which correlates with worsening PLM fibrosis.

Moreover, there are six additional interesting miRNAs that have decreased expression in PN42 PLM (Figure 4). These miRNAs with their targets are as follows: miR-484 (Tgfβr3, Fgf1), miR-455-3p (HB-EGF), miR-130a-3p (Tgfβ2, Tgfβr1, Tnf, Wnt1, Pparγ), miR-677-5p (Col15a1), miR-106b-5p and miR-93-5p (Fgf4, Vegfa, Stat3, Mapk4, Mapk9, Hif1α, Pparα, Col4a3, Col4a4). Tgfβ and Tgfβr are integral to the processing of fibrosis, but are involved in late stages of progressive fibrosis[35]. HB-EGF is a member of the EGF family of proteins and is produced by monocytes and macrophages[36,37]. Recently, high urinary levels of HB-EGF are discovered in the urine of patients with severe PKD[36-38]. Stat3 plays an important role in the pathogenesis of PKD[39,40]. Hif1 has roles in angiogenesis, fibrosis, and is closely tied to local hypoxia[35], which may be the direct result of expanding cystic lesions.

Furthermore, PLM miRNAs with increased expression at PN42 are shown in Figure 4A and their predicted targets are as follows: miR-466d-3p (Smad7), miR-

542-3p (Bmp7), miR-96-5p (βRaf, Nox4), miR-186-5p and miR-329-3p (Usf2) miR-762 (Cx3cl1), miR-155-5p (Socs1, Csf1r), and miR-331-3p (Mmp13). Smad7 inhibits TGF-β signaling by preventing formation of Smad2/Smad4 complexes[35,41]. BMP7 reduces extracellular matrix formation and hence fibrosis[35]. With increased expression of miRNAs, the targets Smad 7 and BMP7 are expected to decrease and hence promote fibrosis. Along with these miRNAs, there are many other novel miRNAs that should be considered for further investigation.

Realizing that all forms of fibrosis eventually involve the TGF-β pathway, we anticipated we would see a few unique differences in miRNA profiles at PN28, the initiation point of fibrosis. We were surprised by the degree of difference and the fact that some were maintained at least through PN42, as seen in Figure 3. Some changes may reflect differences in canonical and non-canonical TGF-β signaling cascades. However, the majority of differences are not likely due to different TGF-β pathways but rather due to differences in methodology. Other changes may reflect key differences in methodology utilized in this study.

A dilution effect created by using an organ with 26 different cell types must be considered when examining miRNAs in whole kidney samples. This has huge implications in the pursuit of therapeutic interventions. The heat map in Figure 2 demonstrates that while the identification of miRNAs that change may be the same with both techniques, the direction of change for some miRNAs goes in opposite directions. This could lead to a situation where a therapy based on whole organ analysis could exacerbate the disease. More importantly, LCM-obtained tissue is expected to represent the local pathology of interest that is being studied.

Fibrosis seen in this ADPKD model is initially localized to discrete areas between multiple cysts, which then expand with the progression of disease. The PLM in which fibrosis occurs undergoes multiple molecular and cellular changes with disease progression. The PLM areas isolated by LCM include locally proliferating cells that likely have key roles in the process of fibrosis. The changes preceding early fibrosis in the PLM of ADPKD kidneys act as a trigger factor that then stimulate cells locally to lay down collagenous extracellular matrix, which causes fibrosis. The isolation of these areas with LCM, as well as examining them at various stages before and after the onset of fibrosis, offers unique insight into this dynamic microenvironment.

Further work is required to identify the phenotypes of these cells and their specific roles. A large number of cells in PLM tissue from ADPKD are phenotypically identified as macrophages. Their role in fibrosis has been well studied and reported[42]. Some or many of these PLM miRNA changes may be directly or indirectly related to macrophage changes that then drive the process of fibrosis. miRNAs are known to modulate macrophage activation and miRNAs are shown to be induced by hypoxia/ischemia. With cyst expansion and compression of parenchyma between these expanding cysts, local hypoxia and ischemic changes can be expected early in the disease course of ADPKD. Whether such hypoxic/ischemic changes drive the early changes in the cellular make-up of the peri-cystic interstitium and drive PLM miRNA changes remain to be investigated.

In conclusions, this study identifies a unique interstitial miRNA signature that drives fibrosis in the new *mcwPkd1*$^{nl/nl}$ model of ADPKD. Such changes in miRNA profiles in ADPKD PLM obtained by LCM provide unique insight into signaling in local areas where fibrosis begins. These PLM miRNA changes are not seen in whole kidney miRNA analysis. These PLM miRNAs have unique predicted targets, and some have established roles in hypoxia, proliferation, angiogenesis and fibrosis. Many of the LCM miRNAs identified are unique and represent new candidates for further study. This approach identifies novel future molecular and therapeutic targets. Further cell-specific miRNA expression studies will provide valuable information in further identifying potential therapeutic targets of fibrosis in ADPKD.

ARTICLE HIGHLIGHTS

Research background

Autosomal dominant polycystic kidney disease (ADPKD) is the most common genetic renal condition, with an incidence of 1 in 500 to 1000 individuals. ADPKD affects approximately 750000 people in the United States and 12.5 million people worldwide. Nearly 50% of ADPKD patients will develop kidney failure that requires dialysis or transplantation. To date, clinical trials targeting cyst growth (epithelial proliferation) have been largely ineffective in improving or slowing the decline in renal function, despite reducing epithelial proliferation and total kidney volume (TKV). Tolvaptan, the most promising therapy to date, has an estimated cost of $744100 per year per quality-adjusted life-year gained compared with standard care.

Research motivation

In ADPKD, as fluid-filled cysts develop and enlarge, a peri-cystic local microenvironment (PLM) is created between the cysts, which become fibrotic over time. TKV decreases with such fibrotic changes and has a strong correlation with loss of renal function. Despite this connection between fibrosis and end-stage renal disease (ESRD), there is no experimental or FDA-approved therapy that specifically targets fibrosis in ADPKD.

Research objectives

To investigate miRNA expression in PLM between cysts that become fibrotic as disease progresses.

Research methods

We employed LCM to analyze the miRNA profile of PLM at PN21, prior to any morphometric sign of fibrosis (trichrome stain), and at two time points of increasing degrees of fibrotic severity at PN28 (initiation) and PN42 (progression). These results were compared to age-matched expression profiles of whole kidney analysis of the miRNA expression profile.

Research results

The most striking result of these studies was the difference in miRNA profiles from PLM and whole kidney, as shown in cluster heat maps. The expression of miRNAs in the PLM was significantly distinct when compared to whole kidney expression.

Research conclusions

Relying on whole kidney analysis may lead one to pursue not only the wrong

miRNA, but may also lead to targeting a miRNA or protein that exacerbates the disease process you are trying to ameliorate. Therefore, published data that relies upon whole kidney transcriptomic analysis should be viewed with careful skepticism. Identification of the molecular and cellular changes in the PLM will lead to new therapeutic targets, with the potential to prevent the initiation or slow the progression of fibrosis.

Research perspectives

This study presents a unique approach to identify novel molecular and therapeutic targets that initiate and drive interstitial fibrosis in ADPKD. The use of therapies targeting fibrosis alone or in combination with therapies targeting epithelial proliferation will dramatically improve the quality of life of ADPKD patients by extending the time to ESRD.

ACKNOWLEDGMENTS

The authors thank Nick Kampa and Emma Schwasinger for their dedication and excellent technical skills that made these experiments possible. The authors also thank Dr. Dorien Peters for providing *Pkd1*$^{(nl/nl)}$ mice to develop the unique *mcwPkd1*$^{(nl/nl)}$ model as described.

REFERENCES

1 **Li Y**, Kowdley KV. MicroRNAs in common human diseases. *Genomics Proteomics Bioinformatics* 2012; **10**: 246-253 [PMID: 23200134 DOI: 10.1016/j.gpb.2012.07.005]

2 **Bae K**, Park B, Sun H, Wang J, Tao C, Chapman AB, Torres VE, Grantham JJ, Mrug M, Bennett WM, Flessner MF, Landsittel DP, Bae KT; Consortium for Radiologic Imaging Studies of Polycystic Kidney Disease (CRISP). Segmentation of individual renal cysts from MR images in patients with autosomal dominant polycystic kidney disease. *Clin J Am Soc Nephrol* 2013; **8**: 1089-1097 [PMID: 23520042 DOI: 10.2215/CJN.10561012]

3 **Ong AC**, Devuyst O, Knebelmann B, Walz G; ERA-EDTA Working Group for Inherited Kidney Diseases. Autosomal dominant polycystic kidney disease: the changing face of clinical management. *Lancet* 2015; **385**: 1993-2002 [PMID: 26090645 DOI: 10.1016/S0140-6736(15)60907-2]

4 **Porath B**, Gainullin VG, Cornec-Le Gall E, Dillinger EK, Heyer CM, Hopp K, Edwards ME, Madsen CD, Mauritz SR, Banks CJ, Baheti S, Reddy B, Herrero JI, Bañales JM, Hogan MC, Tasic V, Watnick TJ, Chapman AB, Vigneau C, Lavainne F, Audrézet MP, Ferec C, Le Meur Y, Torres VE; Genkyst Study Group, HALT Progression of Polycystic Kidney Disease Group; Consortium for Radiologic Imaging Studies of Polycystic Kidney Disease, Harris PC. Mutations in GANAB, Encoding the Glucosidase Ⅱα Subunit, Cause Autosomal-Dominant Polycystic Kidney and Liver Disease. *Am J Hum Genet* 2016; **98**: 1193-1207 [PMID: 27259053 DOI: 10.1016/j.ajhg.2016.05.004]

5 **Harris PC**, Torres VE. Polycystic kidney disease. *Annu Rev Med* 2009; **60**: 321-337 [PMID: 18947299 DOI: 10.1146/annurev.med.60.101707.125712]

6 **Torres VE**. Therapies to slow polycystic kidney disease. *Nephron Exp Nephrol* 2004; **98**: e1-e7 [PMID: 15361692 DOI: 10.1159/000079926]

7 **Pei Y**, Watnick T. Diagnosis and screening of autosomal dominant polycystic kidney disease. *Adv Chronic Kidney Dis* 2010; **17**: 140-152 [PMID: 20219617 DOI: 10.1053/j.ackd.2009.12.001]

8 **Torres VE**, King BF, Chapman AB, Brummer ME, Bae KT, Glockner JF, Arya K, Risk D, Felmlee JP, Grantham JJ, Guay-Woodford LM, Bennett WM, Klahr S, Meyers CM, Zhang X, Thompson PA, Miller JP; Consortium for Radiologic Imaging Studies of Polycystic Kidney Disease (CRISP). Magnetic resonance measurements of renal blood flow and disease progression in autosomal dominant polycystic kidney disease. *Clin J Am Soc Nephrol* 2007; **2**: 112-120 [PMID: 17699395 DOI: 10.2215/CJN.00910306]

9 **Bae KT**, Tao C, Zhu F, Bost JE, Chapman AB, Grantham JJ, Torres VE, Guay-Woodford LM, Meyers CM, Bennett WM; Consortium for Radiologic Imaging Studies Polycystic Kidney Disease. MRI-based kidney volume measurements in ADPKD: reliability and effect of gadolinium enhancement. *Clin J Am Soc Nephrol* 2009; **4**: 719-725 [PMID: 19339416 DOI: 10.2215/CJN.03750708]

10 **Chapman AB**, Wei W. Imaging approaches to patients with polycystic kidney disease. *Semin Nephrol* 2011; **31**: 237-244 [PMID: 21784272 DOI: 10.1016/j.semnephrol.2011.05.003]

11 **Norman J**. Fibrosis and progression of autosomal dominant polycystic kidney disease (ADPKD). *Biochim Biophys Acta* 2011; **1812**: 1327-1336 [PMID: 21745567 DOI: 10.1016/j.bbadis.2011.06.012]

12 **Swenson-Fields KI**, Vivian CJ, Salah SM, Peda JD, Davis BM, van Rooijen N, Wallace DP, Fields TA. Macrophages promote polycystic kidney disease progression. *Kidney Int* 2013; **83**: 855-864 [PMID: 23423256 DOI: 10.1038/ki.2012.446]

13 **Mun H**, Park JH. Inflammation and Fibrosis in ADPKD. *Adv Exp Med Biol* 2016; **933**: 35-44 [PMID: 27730433 DOI: 10.1007/978-981-10-2041-4_4]

14 **Grantham JJ**, Cook LT, Torres VE, Bost JE, Chapman AB, Harris PC, Guay-Woodford LM, Bae KT. Determinants of renal volume in autosomal-dominant polycystic kidney disease. *Kidney Int* 2008; **73**: 108-116 [PMID: 17960141 DOI: 10.1038/sj.ki.5002624]

15 **Raman A**, Reif GA, Dai Y, Khanna A, Li X, Astleford L, Parnell SC, Calvet JP, Wallace DP. Integrin-Linked Kinase Signaling Promotes Cyst Growth and Fibrosis in Polycystic Kidney Disease. *J Am Soc Nephrol* 2017; **28**: 2708-2719 [PMID: 28522687 DOI: 10.1681/ASN.2016111235]

16 **Karihaloo A**, Li X. Role of Inflammation in Polycystic Kidney Disease. In: Li X, editor. Polycystic Kidney Disease. Brisbane (AU): Codon Publications, 2015: Chapter 14 [PMID: 27512776 DOI: 10.15586/codon.pkd.2015.ch14]

17 **Li JY**, Yong TY, Michael MZ, Gleadle JM. Review: The role of microRNAs in kidney disease. *Nephrology (Carlton)* 2010; **15**: 599-608 [PMID: 20883280 DOI: 10.1111/j.1440-1797.2010.01363.x]

18 **Patel V**, Noureddine L. MicroRNAs and fibrosis. *Curr Opin Nephrol Hypertens* 2012; **21**: 410-416 [PMID: 22622653 DOI: 10.1097/MNH.0b013e328354e559]

19 **Patel V**, Williams D, Hajarnis S, Hunter R, Pontoglio M, Somlo S, Igarashi P. miR-17~92 miRNA cluster promotes kidney cyst growth in polycystic kidney disease. *Proc Natl Acad Sci U S A* 2013; **110**: 10765-10770 [PMID: 23759744 DOI: 10.1073/pnas.1301693110]

20 **Hajarnis SS**, Patel V, Aboudehen K, Attanasio M, Cobo-Stark P, Pontoglio M, Igarashi P. Transcription Factor Hepatocyte Nuclear Factor-1β (HNF-1β) Regulates MicroRNA-200 Expression through a Long Noncoding RNA. *J Biol Chem* 2015; **290**: 24793-24805 [PMID: 26292219 DOI: 10.1074/jbc.M115.670646]

21 **Lakhia R**, Hajarnis S, Williams D, Aboudehen K, Yheskel M, Xing C, Hatley ME, Torres VE, Wallace DP, Patel V. MicroRNA-21 Aggravates Cyst Growth in a Model of Polycystic Kidney Disease. *J Am Soc Nephrol* 2016; **27**: 2319-2330 [PMID: 26677864 DOI: 10.1681/ASN.2015060634]

22 **Liang M**, Liu Y, Mladinov D, Cowley AW Jr, Trivedi H, Fang Y, Xu X, Ding X, Tian Z. MicroRNA: a new frontier in kidney and blood pressure research. *Am J Physiol Renal Physiol* 2009; **297**: F553-F558 [PMID: 19339633 DOI: 10.1152/ajprenal.00045.2009]

23 **Wahid F**, Shehzad A, Khan T, Kim YY. MicroRNAs: synthesis, mechanism, function, and recent clinical trials. *Biochim Biophys Acta* 2010; **1803**: 1231-1243 [PMID: 20619301 DOI: 10.1016/j.bbamcr.2010.06.013]

24 **Alberti C**, Cochella L. A framework for understanding the roles of miRNAs in animal development. *Development* 2017; **144**: 2548-2559 [PMID: 28720652 DOI: 10.1242/dev.146613]

25 **Christopher AF**, Kaur RP, Kaur G, Kaur A, Gupta V, Bansal P. MicroRNA therapeutics: Discovering novel targets and developing specific therapy. *Perspect Clin Res* 2016; **7**: 68-74 [PMID: 27141472 DOI: 10.4103/2229-3485.179431]

26 **Vettori S**, Gay S, Distler O. Role of MicroRNAs in Fibrosis. *Open Rheumatol J* 2012; **6**: 130-139 [PMID: 22802911 DOI: 10.2174/1874312901206010130]

27 **Lantinga-van Leeuwen IS**, Dauwerse JG, Baelde HJ, Leonhard

WN, van de Wal A, Ward CJ, Verbeek S, Deruiter MC, Breuning MH, de Heer E, Peters DJ. Lowering of Pkd1 expression is sufficient to cause polycystic kidney disease. *Hum Mol Genet* 2004; **13**: 3069-3077 [PMID: 15496422 DOI: 10.1093/hmg/ddh336]

28 **Tan YC**, Blumenfeld J, Rennert H. Autosomal dominant polycystic kidney disease: genetics, mutations and microRNAs. *Biochim Biophys Acta* 2011; **1812**: 1202-1212 [PMID: 21392578 DOI: 10.1016/j.bbadis.2011.03.002]

29 **Patel V**, Hajarnis S, Williams D, Hunter R, Huynh D, Igarashi P. MicroRNAs regulate renal tubule maturation through modulation of Pkd1. *J Am Soc Nephrol* 2012; **23**: 1941-1948 [PMID: 23138483 DOI: 10.1681/ASN.2012030321]

30 **Hajarnis S**, Lakhia R, Yheskel M, Williams D, Sorourian M, Liu X, Aboudehen K, Zhang S, Kersjes K, Galasso R, Li J, Kaimal V, Lockton S, Davis S, Flaten A, Johnson JA, Holland WL, Kusminski CM, Scherer PE, Harris PC, Trudel M, Wallace DP, Igarashi P, Lee EC, Androsavich JR, Patel V. microRNA-17 family promotes polycystic kidney disease progression through modulation of mitochondrial metabolism. *Nat Commun* 2017; **8**: 14395 [PMID: 28205547 DOI: 10.1038/ncomms14395]

31 **Xu X**, Kriegel AJ, Liu Y, Usa K, Mladinov D, Liu H, Fang Y, Ding X, Liang M. Delayed ischemic preconditioning contributes to renal protection by upregulation of miR-21. *Kidney Int* 2012; **82**: 1167-1175 [PMID: 22785173 DOI: 10.1038/ki.2012.241]

32 **Kriegel AJ**, Liu Y, Liu P, Baker MA, Hodges MR, Hua X, Liang M. Characteristics of microRNAs enriched in specific cell types and primary tissue types in solid organs. *Physiol Genomics* 2013; **45**: 1144-1156 [PMID: 24085797 DOI: 10.1152/physiolgenomics.00090.2013]

33 **Kriegel AJ**, Baker MA, Liu Y, Liu P, Cowley AW Jr, Liang M. Endogenous microRNAs in human microvascular endothelial cells regulate mRNAs encoded by hypertension-related genes. *Hypertension* 2015; **66**: 793-799 [PMID: 26283043 DOI: 10.1161/HYPERTENSIONAHA.115.05645]

34 **Harris PC**, Torres VE. Genetic mechanisms and signaling pathways in autosomal dominant polycystic kidney disease. *J Clin Invest* 2014; **124**: 2315-2324 [PMID: 24892705 DOI: 10.1172/JCI72272]

35 **Liu Y**. Renal fibrosis: new insights into the pathogenesis and therapeutics. *Kidney Int* 2006; **69**: 213-217 [PMID: 16408108 DOI: 10.1038/sj.ki.5000054]

36 **Wei J**, Besner GE. M1 to M2 macrophage polarization in heparin-binding epidermal growth factor-like growth factor therapy for necrotizing enterocolitis. *J Surg Res* 2015; **197**: 126-138 [PMID: 25913486 DOI: 10.1016/j.jss.2015.03.023]

37 **Harskamp LR**, Gansevoort RT, Boertien WE, van Oeveren W, Engels GE, van Goor H, Meijer E. Urinary EGF Receptor Ligand Excretion in Patients with Autosomal Dominant Polycystic Kidney Disease and Response to Tolvaptan. *Clin J Am Soc Nephrol* 2015; **10**: 1749-1756 [PMID: 26231191 DOI: 10.2215/CJN.09941014]

38 **Harskamp LR**, Gansevoort RT, van Goor H, Meijer E. The epidermal growth factor receptor pathway in chronic kidney diseases. *Nat Rev Nephrol* 2016; **12**: 496-506 [PMID: 27374915 DOI: 10.1038/nrneph.2016.91]

39 **Talbot JJ**, Shillingford JM, Vasanth S, Doerr N, Mukherjee S, Kinter MT, Watnick T, Weimbs T. Polycystin-1 regulates STAT activity by a dual mechanism. *Proc Natl Acad Sci U S A* 2011; **108**: 7985-7990 [PMID: 21518865 DOI: 10.1073/pnas.1103816108]

40 **Talbot JJ**, Song X, Wang X, Rinschen MM, Doerr N, LaRiviere WB, Schermer B, Pei YP, Torres VE, Weimbs T. The cleaved cytoplasmic tail of polycystin-1 regulates Src-dependent STAT3 activation. *J Am Soc Nephrol* 2014; **25**: 1737-1748 [PMID: 24578126 DOI: 10.1681/ASN.2013091026]

41 **Meng J**, Li L, Zhao Y, Zhou Z, Zhang M, Li D, Zhang CY, Zen K, Liu Z. MicroRNA-196a/b Mitigate Renal Fibrosis by Targeting TGF-β Receptor 2. *J Am Soc Nephrol* 2016; **27**: 3006-3021 [PMID: 26940097 DOI: 10.1681/ASN.2015040422]

42 **Wynn TA**, Ramalingam TR. Mechanisms of fibrosis: therapeutic translation for fibrotic disease. *Nat Med* 2012; **18**: 1028-1040 [PMID: 22772564 DOI: 10.1038/nm.2807]

P- Reviewer: Chang CC, Rangan G **S- Editor**: Wang JL
L- Editor: Filipodia **E- Editor**: Song H

Published by **Baishideng Publishing Group Inc**
7901 Stoneridge Drive, Pleasanton, CA 94588, USA
Telephone: +1-925-223-8242
Fax: +1-925-223-8243
E-mail: bpgoffice@wjgnet.com
Help Desk: http://www.f6publishing.com/helpdesk
http://www.wjgnet.com